

C-metric solution for conformal gravity with a conformally coupled scalar field

Kun Meng¹ and Liu Zhao²

¹ School of Science, Tianjin Polytechnic University,
Tianjin 300387, China

² School of Physics, Nankai University, Tianjin 300071, China
emails: mengkun@tjpu.edu.cn and lzhao@nankai.edu.cn

Abstract

The C-metric solution of conformal gravity with a conformally coupled scalar field is presented. The solution belongs to the class of Petrov type D spacetimes and is conformal to the standard AdS C-metric appeared in vacuum Einstein gravity. For all parameter ranges, we identify some of the physically interesting static regions and the corresponding coordinate ranges. The solution may contain a black hole event horizon, an acceleration horizon, either of which may be cut by the conformal infinity or be hidden behind the conformal infinity. Since the model is conformally invariant, we also discussed the possible effects of the conformal gauge choices on the structure of the spacetime.

1 Introduction

Conformal gravity is a kind of higher curvature gravity which is invariant under conformal transformations. In the simplest form in four spacetime dimensions, its action is consisted of the square of Weyl curvature tensor. Because of the conformal invariance, this model is only sensitive to angles but not to distances. This feels counter intuition since everyone knows that gravity should decrease as the distance increases. On the level of linear perturbations, conformal gravity suffers from the existence of ghost degrees of freedom, which implies vacuum instability. For these reasons, conformal gravity may well be thought of as an unphysical model of gravity. However, as Maldacena pointed out [1], the on-shell action of conformal gravity is identical to that of Einstein gravity in an (A)dS background, and under proper boundary conditions (Neumann boundary conditions), the contribution from the ghost degrees of freedom can be removed. Conversely, the boundary anomaly of five dimensional Einstein gravity yields the action of four dimensional conformal gravity [1], and also, the four dimensional Einstein gravity with a negative cosmological constant regularized with a topological Gauss-Bonnet term

can be reduced on-shell to that of the conformal gravity [2]. Therefore, it is reasonable to take conformal gravity more seriously than just another toy model of gravity.

Maldacena’s arguments on the equivalence between conformal gravity and Einstein gravity are subjects to several limitations. It works only in the classical (or tree-level) regime, only for backgrounds which are Einstein manifolds obeying the Neumann boundary conditions and only in the vacuum sector. When any of these limitations is broken, it is unclear whether we can still treat conformal gravity as an equivalent model of Einstein gravity. Take the matter contribution for instance. When matter sources are present, it is not clear *a priori* whether Einstein manifolds are solutions to the model and whether the boundary conditions proposed by Maldacena can still be applied. For generic matter sources, the answer to these problems might be “no”, because the boundary conditions actually played an important role in breaking the conformal invariance in some way, but the matter source may have already broken the conformal invariance which leaves no room for breaking the conformal invariance in other ways. But there is an interesting class of matter sources, i.e. conformally coupled matter sources, which keeps the conformal invariance of the model. Conformal gravity with conformally coupled matter sources might still provide room for arguments which are analogous to what Maldacena has made in the vacuum sector.

However, an obvious obstacle will emerge when one tries to mimic Maldacena’s arguments in the cases with conformally coupled sources, i.e. sufficient message on the solutions to such cases is a necessary input. Unlike the case of vacuum conformal gravity which is studied extensively in the literature (and it is known that any spacetime that is conformal to an Einstein manifold is a solution [1]), known solutions to conformal gravity with conformally coupled sources are relatively rare. An outstanding exception is conformal gravity with minimally coupled electromagnetic field. For this particular type of conformal invariant matter source, a number of exact solutions with different symmetries have been found [3, 4]. An extension to the case with an additional SU(2) Yang-Mills source has also been found to possess exact AdS black hole solutions [5]. Besides these particular cases, no other solutions to conformal gravity with conformally coupled matter sources have been known, at least to our knowledge.

In this paper, we aim to present exact solutions to conformal gravity with a conformally coupled scalar field (CGCCS model for short). The type of solution which we will present is quite similar to the C-metric which has been known for a long time [6–8] in the context of pure Einstein gravity. The reason that we pay our attention to the C-metric-like solutions is because such solutions capture almost every aspects of classical relativistic spacetimes and therefore can be used as a nontrivial theoretical laboratory for studying relativistic spacetimes. For instance, they contain black holes – actually two black holes accelerating apart – and hence also acceleration horizons [9–11]. They can be easily generalized to bear cosmological constants [12, 14] and/or electromagnetic charge [9]. For Einstein gravity conformally coupled with a scalar field, the C-metric solution was also found [15, 16]. The rotating form of the C-metric is known as Plebanski-Demianski metric [17]. Finally, the black ring solution [18] which appears in five dimensional Einstein gravity contains a Wick-rotated version of the C-metric as a building

block. We hope that the rich structure of the C-metric may also be useful in exploring the possible connections between conformal gravity and Einstein gravity, or in revealing the differences of conformal gravity from Einstein gravity. As a note in passing, let us remark that, even in the vacuum sector, the C-metric solution in conformal gravity has not been explored (though expected to exist). This is in contrast to the situations of non-accelerating black hole solutions which have been studied extensively [4, 5, 19–22].

The paper is organized as follows. In Section 2, we give the action, field equations and the C-metric solution of the CGCCS model. It is shown that the metric we get represents a spacetime which has a non-constant scalar curvature, but is of Petrov class D, just like the standard C-metric in Einstein gravity. Then, in Section 3, we study coordinate ranges and horizon structures of the solution, with emphasis on the determination of the boundaries of the physically interesting static regions (by which we mean the static region outside a black hole event horizon). This section is subdivided into three subsections according to the different values of the scalar self-coupling λ and another parameter e_2 entering the explicit solution of the scalar field. In Section 4 we consider two other conformal gauges and show that the solution we get is conformal to the standard AdS C-metric appeared in vacuum Einstein gravity. Finally, in Section 4, we give some concluding remarks.

2 The model and the solution

Up to a boundary counter term which is irrelevant to our study in this paper, the action of the CGCCS model that we shall study is given as follows:

$$I = \int d^4x \sqrt{-g} \left[\frac{1}{2} \alpha C^{\mu\nu\rho\sigma} C_{\mu\nu\rho\sigma} - \left(\frac{1}{2} g^{\mu\nu} \partial_\mu \Phi \partial_\nu \Phi + \frac{1}{12} \Phi^2 R + \lambda \Phi^4 \right) \right], \quad (1)$$

where C_{abcd} and R are respectively the Weyl tensor and Ricci scalar associated with the spacetime metric g_{ab} , α and λ are dimensionless coupling constants. Note that the coefficient in front of the $\Phi^2 R$ term is fixed by the requirement of conformal invariance under the transformations

$$g_{\mu\nu} \rightarrow \Omega^2(x) g_{\mu\nu}, \quad \Phi \rightarrow \Omega^{-1}(x) \Phi, \quad (2)$$

so, there can be no other free parameters in the model. Note also that, by a field redefinition $\Phi \rightarrow \alpha^{1/2} \Phi$ together with a rescaling of parameter $\lambda \rightarrow \alpha^{-1} \lambda$, the parameter α becomes an overall factor in the action so that it plays no role on the classical level. Therefore, we can set $\alpha = 1$ without loss of generality. In order that the scalar self-interacting potential to be bounded from below, it is necessary to require $\lambda \geq 0$.

The field equations that follow from variations with respect to the metric g_{ab} and to the scalar field Φ are given respectively as

$$B_{\mu\nu} = -T_{\mu\nu}^{(\Phi)}, \quad (3)$$

$$\square \Phi = \frac{1}{6} R \Phi + 4\lambda \Phi^3, \quad (4)$$

where

$$B_{\mu\nu} = 2\nabla^\rho\nabla^\sigma C_{\mu\rho\sigma\nu} + R^{\rho\sigma}C_{\mu\rho\sigma\nu} \quad (5)$$

is the Bach tensor and

$$T_{\mu\nu}^{(\Phi)} = \partial_\mu\Phi\partial_\nu\Phi - \frac{1}{2}g_{\mu\nu}\partial^\rho\Phi\partial_\rho\Phi - \lambda g_{\mu\nu}\Phi^4 + \frac{1}{6}(g_{\mu\nu}\square - \nabla_\mu\nabla_\nu + G_{\mu\nu})\Phi^2 \quad (6)$$

is the stress-energy tensor for the scalar field Φ .

In the spacetime coordinates $x^\mu = (t, y, x, \sigma)$, we take the metric ansatz

$$ds^2 = \frac{1}{A^2(x-y)^2} \left(-F(y)dt^2 + \frac{dy^2}{F(y)} + \frac{dx^2}{G(x)} + G(x)d\sigma^2 \right), \quad (7)$$

and meanwhile assume the scalar field to take the form

$$\Phi(x, y) = \frac{e_1(x-y)}{x+y-e_2}, \quad (8)$$

where A, e_1, e_2 are all constants.

By brute force using *Maple*, we arrive at the following solution:

$$\begin{aligned} G(x) &= \frac{1}{6}C_1x^3 + \frac{1}{2}C_2x^2 + C_3x + C_4, \\ F(y) &= \frac{1}{6}C_1y^3 - \frac{1}{2}(C_1e_2 + C_2)y^2 + \left(\frac{1}{2}C_1e_2^2 + C_2e_2 + C_3 \right) y \\ &\quad - \left(\frac{1}{6}C_1e_2^3 + \frac{1}{2}C_2e_2^2 + C_3e_2 + C_4 - \frac{2e_1^2\lambda}{A^2} \right), \end{aligned} \quad (9)$$

where $C_i (i = 1, \dots, 4)$ are integration constants. Not all of these constants are necessarily important. We can make use of the coordinate transformations to fix some of these constants and reduce the solution to a simpler form. To be more specific, we can use the following 3-parameter coordinate transformations

$$t \rightarrow bt, \quad y \rightarrow aby - c, \quad x \rightarrow abx - c, \quad \sigma \rightarrow b\sigma \quad (10)$$

to fix or constrain three of the four integration constants C_i at the sacrifice of a rescaling of the constant A and a shift and rescaling of the constant e_2 . The constant e_1 is not affected by such operations. In the following, we shall take the liberty of the above coordinate degrees of freedom to set the integration constants C_i to the specific values

$$\begin{aligned} C_1 &= -12mA, & C_2 &= -2, \\ C_3 &= 2mA, & C_4 &= 1, \end{aligned} \quad (11)$$

where m is the only residual free integration constant, which may be chosen to be always positive thanks to the transformation rules (10). Notice that we still denote the rescaled

constant A and the shift-rescaled e_2 by the same symbols. Under the above choice of integration constants, the metric functions $G(x)$ and $F(y)$ can be arranged in the form

$$G(x) = (1-x)(1+x)(1+2mA x), \quad (12)$$

$$F(y) = -[1-(e_2-y)][1+(e_2-y)][1+2mA(e_2-y)] + \frac{2e_1^2\lambda}{A^2}. \quad (13)$$

It is straightforward to observe that

$$F(\xi) = -G(e_2 - \xi) + \frac{2e_1^2\lambda}{A^2}. \quad (14)$$

The metric (7) with $G(x)$ and $F(y)$ given respectively by (12) and (13) looks extremely similar to the C-metric solution of vacuum Einstein gravity, therefore we call this solution the C-metric solution for the CGCCS model. However, there are some significant differences from the standard C-metric in Einstein gravity. Among these, let us point out two major differences:

- Unlike the vacuum C-metric in Einstein gravity, our solution is sourced, sensitive to the scalar field (which can be seen from the appearance of the constants e_1, e_2 and λ in (12) and (13));
- Our solution is not a constant curvature spacetime. By straightforward calculations and some elementary algebraic manipulations, the Ricci scalar of our solution can be written in the following form:

$$R = -24e_1^2\lambda - 2A^2\{(x+y)^2 + 2xy + 6(x+y-e_2)[(2mA-e_2) + mA(e_2(x+y-e_2) - 2xy - e_2^2)]\}.$$

So, it will be interesting to ask whether our solution is conformal to an Einstein manifold. We postpone the answer of this question to Section 4.

In spite of the differences mentioned above, there is a crucial similarity between our solution and the standard C-metric. By choosing the null Newman-Penrose tetrads

$$\begin{aligned} l^\mu &= \frac{1}{\sqrt{2}}(T^\mu + Y^\mu), & n^\mu &= \frac{1}{\sqrt{2}}(T^\mu - Y^\mu), \\ m^\mu &= \frac{1}{\sqrt{2}}(X^\mu + iS^\mu), & \bar{m}^\mu &= \frac{1}{\sqrt{2}}(X^\mu - iS^\mu), \end{aligned}$$

where

$$\begin{aligned} T^\mu &= \left(\frac{A(x-y)}{\sqrt{F(y)}}, 0, 0, 0 \right), & Y^\mu &= \left(0, A(x-y)\sqrt{F(y)}, 0, 0 \right), \\ X^\mu &= \left(0, 0, A(x-y)\sqrt{G(x)}, 0 \right), & S^\mu &= \left(0, 0, 0, \frac{A(x-y)}{\sqrt{G(x)}} \right), \end{aligned}$$

we find that the only nonvanishing projection of the Weyl curvature of our spacetime on the Newman-Penrose null tetrads is

$$\Psi_2 = C_{\mu\nu\rho\sigma} n^\mu m^\nu \bar{m}^\rho l^\sigma = -mA^3(x-y)^2(x+y-e_2).$$

Therefore, our solution is of Petrov type D, just like the standard C-metric in vacuum Einstein gravity.

3 Coordinate ranges and horizon structures

In this section, we would like to analyze some aspects of the structure of the spacetime solution given by eqs. (7), (12) and (13). We will be particularly interested in the understandings about the ranges of the coordinates, the horizon structures and the interpretation of the constant parameters. Essentially we will be following the lines of [11] and that of [23].

According to (13), the root structure of the function $F(y)$ is different for the cases $\lambda = 0$ and $\lambda \neq 0$. In the former case, the function $F(y)$ is already factorized, from which we can read off explicitly the three roots, which are all independent of the constant e_1 . In the latter case, however, the function $F(y)$ is not factorized, and it is more difficult to find its root structure. So, we will proceed differently for these two cases.

3.1 The case $\lambda = 0$

When $\lambda = 0$, $F(y)$ is explicitly factorized, so it is easy get the roots of $F(y)$:

$$y_1 = e_2 - 1, \quad y_2 = e_2 + 1, \quad y_3 = e_2 + \omega^{-1}. \quad (15)$$

Here we have introduced the shorthand notation

$$\omega \equiv 2mA$$

because this expression will appear repeatedly in the forth coming discussions. To fix the order of the three roots, we assume $0 < \omega < 1$ which can always be achieved using the transformations given in (10). Under this assumption, we have

$$y_1 < y_2 < y_3,$$

regardless of what value the constant e_2 takes (provided it is real).

The metric (7) depends explicitly only on two of the four spacetime coordinates (x, y) . Therefore let us first try to determine the physical regions for these two coordinates. Recall that the correct Lorentz signature of the metric (7) requires $G(x) > 0$. This is achieved by setting $-1 < x < 1$, or reparametrized as

$$x = \cos \theta, \quad (0 < \theta < \pi).$$

The alternative choice $x < -\omega^{-1}$ can also yield correct Lorentz signature, but this choice corresponds to an unbounded x coordinate, which is physically uninteresting because x is to be interpreted as one of the angular coordinates. On the other hand, the existence of a static region in the spacetime requires $F(y) > 0$. Rewriting $F(y)$ as

$$F(y) = -\omega(y - y_1)(y - y_2)(y - y_3), \quad (16)$$

it is clear that the condition $F(y) > 0$ requires either $y < y_1$ or $y_2 < y < y_3$. It will become clear shortly that the third root $y = y_3$ of $F(y)$ corresponds to a black hole event horizon. Therefore, the first region $y < y_1$ is physically relatively less interesting because the black hole event horizon is out of reach from this region. The second region $y_2 < y < y_3$ is more interesting following the same consideration. So, for now, let us assume that y takes values in the second region. Finally, due to the overall conformal factor, we know that $x = y$ is the conformal infinity of our spacetime, thus the physical region of the spacetime requires either $y > x$ or $y < x$ but not across $y = x$. In the following, we shall be concentrating exclusively on the physically interesting region $y > x$. The region $y < x$ may also be of some physical interests, but it is out of our main focus in this paper. Depending on the values of e_2 and ω , the static region of the spacetime is bounded by the lines $x = \pm 1$, $y = y_2$, $y = y_3$ and the condition $y > x$. The details are shown in Figs.1 and 2.

In Fig.1, all physically interesting static regions are shaded in darkgray. Some of the pictures in Fig.1 also contain a region shaded in lightgray, which are considered to be unphysical, because they appear on the other side of conformal infinity. The region shaded in darkgray in Fig.1(a) corresponds to the static region outside a black hole. The lower boundary at $y = y_2$ corresponds to a compact acceleration horizon as will become clear later. This case is similar to the de Sitter C-metric in Einstein gravity (cf. Fig.2(a) in ref. [23]) except that the present spacetime has a non-constant scalar curvature. The conformal infinity $y = x$ lies behind the acceleration horizon and is out of reach from this region. The region in darkgray in Fig.1(b) is again a static region outside a black hole, with lower boundary at $y = y_2$ corresponding to an acceleration horizon. The difference from the case of Fig.1(a) lies in that the acceleration horizon hits the conformal infinity at some intermediate value $-1 < x < 1$, so the acceleration horizon cannot be compact in this case. In Fig.1(c), both the upper and lower boundaries of the region shaded in darkgray hits the conformal infinity at some intermediate value of x , so this static region contains a non-compact black hole event horizon and a non-compact acceleration horizon. Unlike the case of Fig.1(c), the case of Fig.1(d) corresponds to a larger ω^{-1} , which makes the upper shaded region to have a compact black hole event horizon but the acceleration horizon lies completely behind the conformal infinity and hence is out of reach from this region. The upper shaded region in Fig.1(e) has a non-compact black hole event horizon as its upper boundary, which hits conformal infinity at some $-1 < x < 1$. The acceleration horizon is beyond reach because it hides behind the conformal infinity. The last figure, Fig.1(f), contains no region shaded in darkgray, which means that there is no physically interesting static region for this set of parameters.

Fig.1 described only the cases for generic values of e_2 and ω^{-1} . However, there are also some particular values of e_2 and ω^{-1} which are not shown, i.e. the cases $e_2 = 0$, $e_2 = -2$

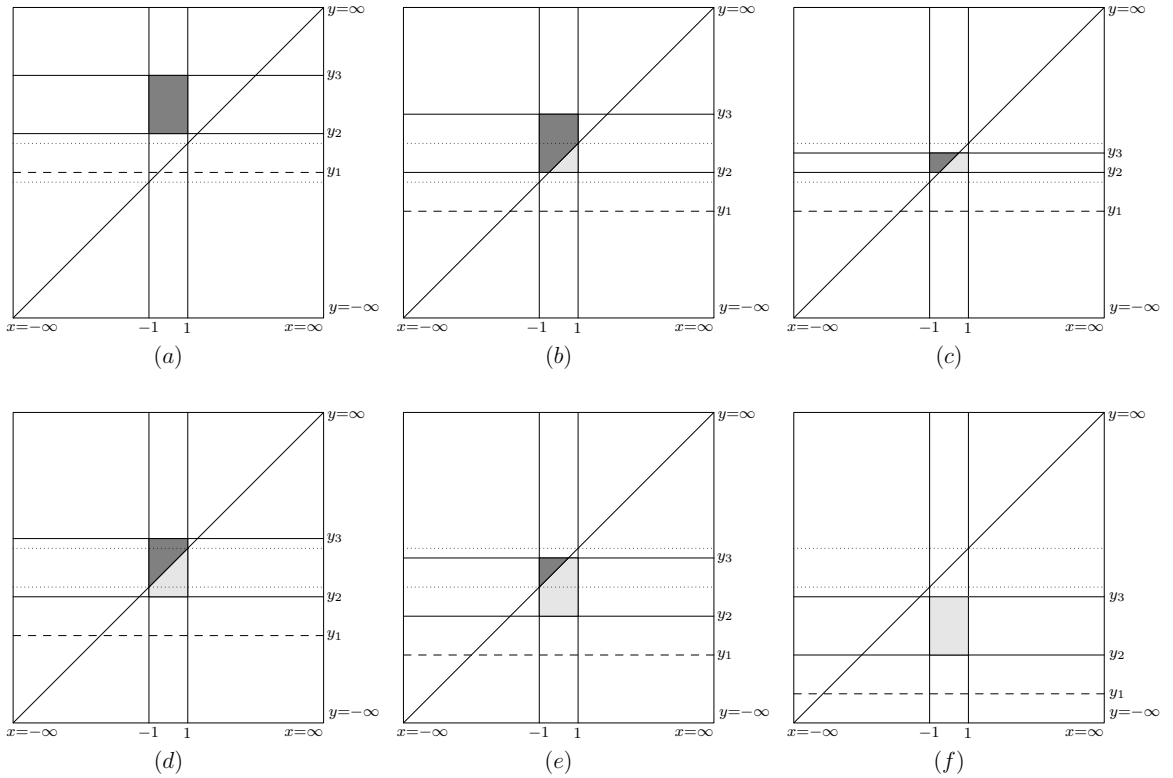


Figure 1: Physically interesting static regions: dotted lines correspond to $y = \pm 1$. (a) $e_2 > 0$; (b) $-2 < e_2 < 0$ and $\omega^{-1} > 1 - e_2$; (c) $-2 < e_2 < 0$ and $\omega^{-1} < 1 - e_2$; (d) $e_2 < -2$ and $\omega^{-1} > 1 - e_2$; (e) $e_2 < -2$ and $-e_2 - 1 < \omega^{-1} < 1 - e_2$; (f) $e_2 < -2$ and $0 < \omega^{-1} < -e_2 - 1$.

and/or $\omega^{-1} = 1 - e_2$. These special cases can be viewed as certain limiting cases of the plots given in Fig.1. Some of these limiting cases are depicted in Fig.2. The limiting case of Fig.1(f) at $y_3 \rightarrow -1$ is not displayed here because this case is physically uninteresting just like Fig.1(f). In all cases displayed in Fig.2, either the black hole event horizon or the acceleration horizon hits the conformal infinity at a single point.

In all cases displayed in Figs.1 and 2 except Fig.1(f), the region bounded by the lines $x = \pm 1$, $y = y_3$, $y = +\infty$ and possibly $y = x$ represents the black hole interior which are non-static. The regions bounded by $x = -1$, $y = y_2$ and $y = x$ in Figs.1(b), 1(c), 2(a) and 2(f) are non-static and non-compact which all hide behind the acceleration horizon at $y = y_2$. Moreover, in Fig.1(a), the region bounded by the lines $x = \pm 1$, $y = y_1$, $y = y_2$ and $y = x$ corresponds also to a non-static and non-compact region, and there is yet another static region bounded by $x = -1$, $y = y_1$ and $y = x$. Here $y = y_1$ may be interpreted as a cosmological horizon (this interpretation of the acceleration horizon is similar to the case of AdS C-metric in Einstein gravity as shown in [12, 13]).

The descriptions made in the last few paragraphs rely heavily on the statements that the root $y = y_3$ corresponds to a black hole event horizon and $y = y_2$ corresponds to an acceleration horizon. Now it is time to justify these statements. For this purpose

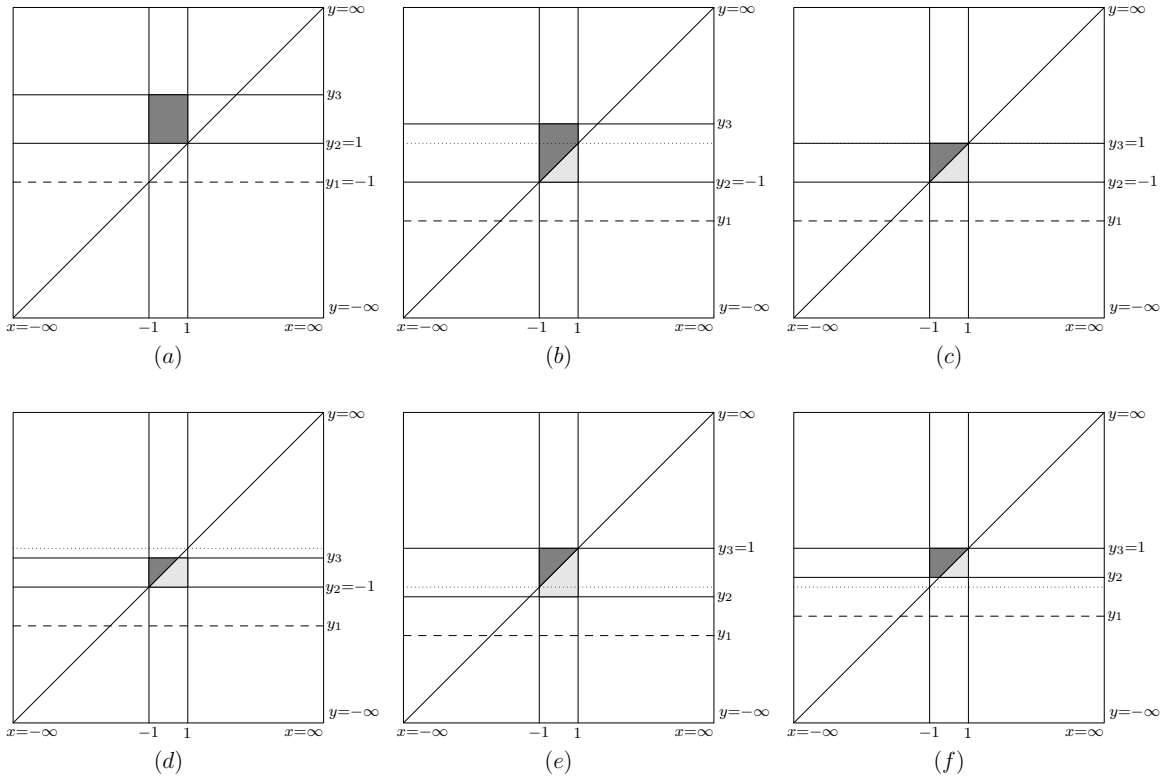


Figure 2: Some of the limiting cases. (a) $e_2 = 0$; (b) $e_2 = -2$ and $\omega^{-1} > 3$; (c) $e_2 = -2$ and $\omega^{-1} = 3$; (d) $e_2 = -2$ and $\omega^{-1} < 3$; (e) $e_2 < -2$ and $\omega^{-1} = 1 - e_2$; (f) $-2 < e_2 < 0$ and $\omega^{-1} = 1 - e_2$.

let us first remark that the curvature invariants such as R , $R_{\mu\nu}R^{\mu\nu}$ and $R_{\mu\nu\rho\sigma}R^{\mu\nu\rho\sigma}$ are all finite at $y = y_i (i = 1, 2, 3)$, though the concrete expressions for the latter two curvature invariants are too lengthy and hence do not worth to be displayed here. This indicates that the roots of $F(y)$ are coordinate singularities, not essential ones. The true curvature singularity arises at $y = \pm\infty$, which can already be seen from the expression of Ricci scalar given in the last section.

To understand the role of the roots of $F(y)$, let us calculate the proper acceleration of a static observer in the spacetime. The static observer is chosen as

$$x^\mu = \left(\frac{A(x-y)}{\sqrt{F(y)}} \eta, y, x, \sigma \right), \quad (17)$$

where $F(y)$ is given in (13) with $\lambda = 0$, η is the proper time, and the spatial coordinates (y, x, σ) are fixed to some constants. The proper velocity of this static observer is

$$v^\mu = \left(\frac{A(x-y)}{\sqrt{F(y)}}, 0, 0, 0 \right), \quad (18)$$

and hence the corresponding proper acceleration reads

$$a^\mu = v^\nu \nabla_\nu v^\mu = A^2(x - y) (0, \beta, \gamma, 0), \quad (19)$$

where

$$\begin{aligned} \beta &= -1 + xy - e_2(x + y - e_2) + Am(x + y + y^3 - 3xy^2) \\ &\quad + Ame_2(-2 + 6xy - 3xe_2 - 3ye_2 + 2e_2^2), \\ \gamma &= -G(x). \end{aligned}$$

Therefore, the norm of the proper acceleration is

$$|a|^2 = g_{\mu\nu} a^\mu a^\nu = A^2 \left(\frac{\beta^2}{F(y)} + G(x) \right). \quad (20)$$

It is important to note that β does not have any common factor with $F(y)$, hence $|a|^2$ diverges at all three roots of $F(y)$. In other words, all roots of $F(y)$ are acceleration horizons if accessible from the static region. Among these, $y = y_1$ is not accessible from the shaded static regions depicted in Figs.1 and 2, so we are left with only two acceleration horizons at $y = y_2$ and $y = y_3$. In the following, we shall make it clear that the root $y = y_3$ is actually a black hole event horizon, so only $y = y_2$ is a pure acceleration horizon.

It should be remarked that the above analysis for the curvature singularity and for the acceleration horizons applies not only to the $\lambda = 0$ case. For $\lambda > 0$, the same analysis still works and the conclusion is unchanged. The only difference lies in that the roots of $F(y)$ may be different and that the expression for β becomes more complicated.

Since the causal character of conformal infinity is an interesting issue, we try to make a clarification on this point. The character of conformal infinity can be studied through the norm of tangent vector of the hypersurface. The tangent vector of conformal infinity is $\Omega_{,\mu}$, where $\Omega = A(x - y)$ and $\Omega = 0$ corresponds to conformal infinity. Since $\Omega = 0$ corresponds to singularity of the spacetime (7), we should calculate the norm of $\Omega_{,\mu}$ in a new spacetime $d\tilde{s}^2 = \Omega^2 ds^2$, where

$$d\tilde{s}^2 = -F(y)dt^2 + \frac{dy^2}{F(y)} + \frac{dx^2}{G(x)} + G(x)d\sigma^2, \quad (21)$$

with $F(y)$ and $G(x)$ given in (12) and (13). Now conformal infinity in spacetime ds^2 corresponds to $\Omega = 0$ hypersurface in spacetime $d\tilde{s}^2$. The norm of $\Omega_{,\mu}$ is

$$\begin{aligned} \Omega_{,\mu}\Omega_{,\nu}\tilde{g}^{\mu\nu} &= -4A^3mx^3 + 6A^3e_2mx^2 + (-2A^2e_2 + 4A^3m - 6A^3e_2^2m)x \\ &\quad + A^2e_2^2 - 2A^3e_2m + 2A^3e_2^3m + 2e_1^2\lambda. \end{aligned} \quad (22)$$

Note that in Einstein gravity norm of the tangent vector of conformal infinity depends only on cosmological constant, i.e., the sign of cosmological constant determines the causal character of conformal infinity uniquely. However, for the C-metric of CGCCS model, norm of the tangent vector of conformal infinity depends on the coordinate x .

In order to determine the sign of the norm (22), we need to find the real roots of the equation $\Omega_{,\mu}\Omega_{,\nu}\tilde{g}^{\mu\nu} = 0$, the character of conformal infinity is different on the two sides of the real roots. Solving the equation $\Omega_{,\mu}\Omega_{,\nu}\tilde{g}^{\mu\nu} = 0$ roughly we have the following three roots

$$\begin{aligned} x_1 &= \frac{e_2}{2} + \frac{X}{6mA^3 2^{2/3}(-Y + \sqrt{4X^3 + Y^2})^{1/3}} - \frac{(-Y + \sqrt{4X^3 + Y^2})^{1/3}}{12mA^3 2^{1/3}}, \\ x_2 &= \frac{e_2}{2} - \frac{(1 + i\sqrt{3})X}{12mA^3 2^{2/3}(-Y + \sqrt{4X^3 + Y^2})^{1/3}} + \frac{(1 - i\sqrt{3})(-Y + \sqrt{4X^3 + Y^2})^{1/3}}{24mA^3 2^{1/3}}, \\ x_3 &= \frac{e_2}{2} - \frac{(1 - i\sqrt{3})X}{12mA^3 2^{2/3}(-Y + \sqrt{4X^3 + Y^2})^{1/3}} + \frac{(1 + i\sqrt{3})(-Y + \sqrt{4X^3 + Y^2})^{1/3}}{24mA^3 2^{1/3}}, \end{aligned} \quad (23)$$

with $X = 24mA^5e_2 - 48m^2A^6 + 36m^2A^6e_2^2$ and $Y = 864m^2A^6e_1^2\lambda$. To find which root is real, we need to consider the sign of $4X^3 + Y^2$. When $4X^3 + Y^2 \geq 0$, it is easy to see that x_1 is real. If one further requires either x_2 or x_3 is real, this would end up with the condition $4X^3 + Y^2 = 0$. Thus for $4X^3 + Y^2 = 0$ we have two real roots (x_2 equals to x_3 in this case), and for $4X^3 + Y^2 > 0$ we have only one real root. For $4X^3 + Y^2 = 0$ the two real roots are

$$x_1 = \frac{e_2}{2} + \frac{(Y/2)^{1/3}}{6mA^3}, \quad x_2 = \frac{e_2}{2} - \frac{(Y/2)^{1/3}}{12mA^3}. \quad (24)$$

When $4X^3 + Y^2 < 0$, one notes that X is negative and the modulus of $-Y + \sqrt{4X^3 + Y^2}$ is $2|X|^{3/2}$, thus we may write

$$-Y + \sqrt{4X^3 + Y^2} = 2|X|^{3/2}e^{i\theta}, \quad (25)$$

and $(-Y + \sqrt{4X^3 + Y^2})^{1/3} = 2^{1/3}|X|^{1/2}e^{i(\theta+2n\pi)/3}$, where θ is dependent on the values of X and Y and hence also on e_1 and e_2 . After a little calculation, one will find that x_2 and x_3 are real and equal to each other, i.e.,

$$x_2 = x_3 = \frac{e_2}{2} + \frac{|X|^{1/2} \cos[(\pi + \theta + 2n\pi)/3]}{6mA^3}. \quad (26)$$

x_1 is real too, which can also be written as

$$x_1 = \frac{e_2}{2} - \frac{|X|^{1/2} \cos[(\theta - 2n\pi)/3]}{6mA^3}. \quad (27)$$

In any case, the position of the real roots of the right hand side of (22) is dependent on the values of e_1 and e_2 , and provided the real roots are sitting in between $x = \pm 1$, the character of the conformal infinity will change (either from timelike to spacelike or vice versa) on the two sides of the single root. For double roots the character of the conformal infinity on both sides are the same, and it changes into lightlike at the roots.

Now let us come back to the $\lambda = 0$ case and introduce the following coordinate transformations

$$x = \cos \theta, \quad y - e_2 = \frac{1}{Ar}, \quad t = A\tau. \quad (28)$$

In terms of these new coordinates, the metric (7) can be written as

$$ds^2 = \frac{1}{[1 - Ar(\cos \theta - e_2)]^2} \left[-Q(r) d\tau^2 + \frac{dr^2}{Q(r)} + r^2 \left(\frac{d\theta^2}{P(\theta)} + P(\theta) \sin^2 \theta d\sigma^2 \right) \right], \quad (29)$$

where

$$Q(r) = (1 - A^2 r^2) \left(1 - \frac{2m}{r} \right), \quad P(\theta) = 1 + 2mA \cos \theta. \quad (30)$$

When $A = 0$, the metric (29) degenerates into that of the Schwarzschild black hole, with $r = 2m$ being the event horizon. Note that the root $r = 2m$ of $Q(r)$ corresponds to the root $y = y_3$ of $F(y)$, so $y = y_3$ needs to be the black hole event horizon even at $A \neq 0$.

To interpret the physical meaning of the constant A , let us consider the weak field limit $m \rightarrow 0$. In this limit, the second factor in (20) becomes a constant which is independent of A . Thus, *the proper acceleration of any static observer in the weak field limit is proportional to A .*

It remains to determine the ranges of the coordinates t, σ . As a timelike coordinate, t is unconstrained in the static region, so $-\infty < t < +\infty$. As for the angular coordinate σ , let us examine the possible deficit angles around the $\theta = 0$ and $\theta = \pi$ half axes of the $t = \text{const}$ and $r = \text{const}$ hypersurface. Assuming $\sigma \in [-\pi C, \pi C]$, the circumference to radius ratios for the infinitesimal circles around the above two half axes are respectively

$$\lim_{\theta \rightarrow 0} \frac{2\pi C P(\theta) \sin \theta}{\theta} = 2\pi C(1 + 2mA), \quad (\theta = 0), \quad (31)$$

$$\lim_{\theta \rightarrow \pi} \frac{2\pi C P(\theta) \sin \theta}{\pi - \theta} = 2\pi C(1 - 2mA), \quad (\theta = \pi). \quad (32)$$

Thus, there exist different conical singularities for the $\theta = 0$ and $\theta = \pi$ half axes. The conical singularity at the $\theta = 0$ pole can be canceled by taking $C = 1/(1 + 2mA)$. Then the deficit angle at $\theta = \pi$ is $8\pi Am/(1 + 2mA)$. The deficit angle at the $\theta = \pi$ pole is interpreted as a semi-infinite cosmic string along the $\theta = \pi$ half axes which drags and accelerates a Schwarzschild-like black hole along the axis [11].

3.2 The case $\lambda > 0$ with $e_2 = 0$

The situation for $\lambda > 0$ is much more complicated than the case $\lambda = 0$, because $F(y)$ is no longer explicitly factorized. To make things easier, let us first consider the degenerated case $e_2 = 0$.

When $\lambda > 0$ and $e_2 = 0$, eqs.(12)-(14) can be rewritten as

$$G(x) = (1 - x)(1 + x)(1 + \omega x), \quad (33)$$

$$F(y) = -(1 + y)(1 - y)(1 - \omega y) + \frac{2e_1^2 \lambda}{A^2}. \quad (34)$$

In this case, it will be convenient to introduce a coordinate reflection $y \rightarrow \tilde{y} = -y$, after which the metric becomes

$$ds^2 = \frac{1}{A^2(x + \tilde{y})^2} \left(\mathcal{F}(\tilde{y})dt^2 - \frac{d\tilde{y}^2}{\mathcal{F}(\tilde{y})} + \frac{dx^2}{\mathcal{G}(x)} + \mathcal{G}(x)d\sigma^2 \right), \quad (35)$$

where

$$\mathcal{G}(\xi) = (1 - \xi)(1 + \xi)(1 + \omega\xi), \quad (36)$$

$$\mathcal{F}(\xi) = (1 - \xi)(1 + \xi)(1 + \omega\xi) - X, \quad (37)$$

$$X \equiv \frac{2e_1^2\lambda}{A^2} > 0,$$

and clearly

$$\mathcal{F}(\xi) = \mathcal{G}(\xi) - X. \quad (38)$$

According to (38), $\mathcal{F}(\xi)$ differs from $\mathcal{G}(\xi)$ by a negative constant shift. Meanwhile, $\mathcal{G}(\xi)$ has three explicit real roots thanks to (36). Since the function $\mathcal{F}(\xi)$ is a polynomial of degree 3 in ξ , it may have one, two or three real roots depending on the amount of shift, X . We will be mostly interested in the case when $\mathcal{F}(\xi)$ has three real roots, because this is the case with as many horizons as possible. The other two cases will be discussed at the end of this subsection.

In order to determine the condition for $\mathcal{F}(\xi)$ to have three real roots, we first identify its minimum and maximum, which read

$$\mathcal{F}_{\min} = -\frac{\sqrt{12\omega^2 + 1} + 6\omega^2 (2\sqrt{12\omega^2 + 1} + 9X - 6) + 1}{54\omega^2},$$

$$\mathcal{F}_{\max} = \frac{\sqrt{12\omega^2 + 1} + 6\omega^2 (2\sqrt{12\omega^2 + 1} - 9X + 6) - 1}{54\omega^2}.$$

$\mathcal{F}(\xi)$ will have three real roots if and only if $\mathcal{F}_{\min} < 0$ and $\mathcal{F}_{\max} > 0$. Recalling that $X > 0$, we find that in order for $\mathcal{F}(\xi)$ to have three real roots, the value of X must be constrained to be within the range

$$X \in \left(0, \frac{12(\sqrt{12\omega^2 + 1} + 3)\omega^2 + \sqrt{12\omega^2 + 1} - 1}{54\omega^2} \right).$$

Now assuming that the above condition is fulfilled. Then $\mathcal{F}(\xi)$ can be written in a factorized form¹

$$\mathcal{F}(\xi) = (\xi - a)(\xi - b)(k_0 + k_1\xi). \quad (39)$$

¹Notice that the parameters a, b, c used here and below has nothing to do with those appeared in (10).

Similarly we rewrite $\mathcal{G}(x)$ as

$$\mathcal{G}(\xi) = (\xi - 1)(\xi + 1)(p_0 + p_1\xi), \quad (40)$$

where of course $p_0 = -1, p_1 = -\omega$. Comparing eqs.(39) and (40) with (36) and (37), we get

$$\begin{aligned} p_0 &= \Xi [-(a+b)^2 + ab + 1] = -1, & p_1 &= \Xi(a+b) = -\omega, \\ k_0 &= \Xi(1+ab), & k_1 &= \Xi(a+b), \end{aligned} \quad (41)$$

where

$$\Xi = \frac{2\lambda e_1^2}{A^2(a^2 - 1)(1 - b^2)} = \frac{X}{(a^2 - 1)(1 - b^2)}. \quad (42)$$

Note that we can in principle determine a, b in terms of λ, A, e_1, ω using the above relations. Now since p_0, p_1, k_0, k_1 have a common factor Ξ , we can pick out this common factor and rewrite the metric as

$$ds^2 = \frac{1}{\Xi A^2(x + \tilde{y})^2} \left(\tilde{\mathcal{F}}(\tilde{y})d\tilde{t}^2 - \frac{d\tilde{y}^2}{\tilde{\mathcal{F}}(\tilde{y})} + \frac{dx^2}{\tilde{\mathcal{G}}(x)} + \tilde{\mathcal{G}}(x)d\tilde{\sigma}^2 \right), \quad (43)$$

where $\tilde{t} = \Xi t, \tilde{\sigma} = \Xi \sigma$ and

$$\tilde{\mathcal{G}}(\xi) = \Xi^{-1}\mathcal{G}(\xi) = (\xi - 1)(\xi + 1)[(a+b)(\xi - a - b) + ab + 1], \quad (44)$$

$$\tilde{\mathcal{F}}(\xi) = \Xi^{-1}\mathcal{F}(\xi) = (\xi - a)(\xi - b)[(a+b)\xi + ab + 1]. \quad (45)$$

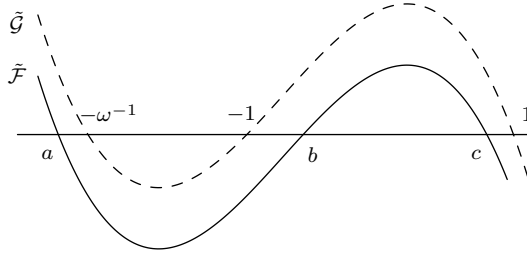


Figure 3: $\tilde{\mathcal{F}}(\xi)$ differs from $\tilde{\mathcal{G}}(\xi)$ by a negative constant shift

The metric (43) is invariant under the following two sets of discrete transformations:

$$(1) \quad \tilde{y} \rightarrow -\tilde{y}, \quad x \rightarrow -x, \quad a \rightarrow -a, \quad b \rightarrow -b, \quad (46)$$

$$(2) \quad a \leftrightarrow b. \quad (47)$$

These symmetries allow us to take, without loss of generality, $a+b < 0$ and $a < b$. Thus we have $a < 0$. Moreover, it follows from (38) that

$$\tilde{\mathcal{G}}(\xi) - \tilde{\mathcal{F}}(\xi) = \Xi^{-1}X = (a^2 - 1)(1 - b^2). \quad (48)$$

From (44) it is evident that the roots of $\tilde{\mathcal{G}}(x)$ coincides with those of $\mathcal{G}(x)$, i.e. $x = \pm 1, -\omega^{-1}$. Just like the $\lambda = 0$ case, we restrict $-1 < x < 1$, so that $\tilde{\mathcal{G}}(x) > 0$. Under this condition, the correct Lorentz signature of the metric (43) requires $\Xi > 0$ and $\tilde{\mathcal{F}}(\tilde{y}) < 0$ in the static region. Since we already have $\lambda > 0$, the only possibility is to set $(a^2 - 1)(1 - b^2) > 0$ in order that the condition $\Xi > 0$ is satisfied. On the other hand, from (45) we can read off the three real roots of $\tilde{\mathcal{F}}(\tilde{y})$, i.e. $\tilde{y} = a, b$ and $\tilde{y} = c \equiv -\frac{ab+1}{a+b}$. It then follows from (48) that the roots of $\tilde{\mathcal{G}}(\xi)$ and $\tilde{\mathcal{F}}(\xi)$ are ordered as

$$a < -\omega^{-1} < -1 < b < c < 1, \quad (49)$$

as can be inferred from Fig.3. In the static region, we need to have $\tilde{\mathcal{F}}(\tilde{y}) < 0$, therefore, this region is bounded by $a < \tilde{y} < b$ or $\tilde{y} > c$. Besides the two pairs $x = \pm 1, \tilde{y} = a, b$ of boundaries, the static region is also constrained by the conformal infinity which is now defined by $x + \tilde{y} = 0$. Assuming $\tilde{y} < -x$ (which is equivalent to $y > x$ in the last subsection), we can depict the static region of the $\lambda > 0, e_2 = 0$ case of our solution as the dark shaded region in Fig.4. In this case, the region $-1 < x < 1, -\infty < \tilde{y} < a$ represents the black hole interior. The region bounded by $x = -1, \tilde{y} = b, \tilde{y} = c$ and $\tilde{y} = -x$ corresponds to a non-static region with $\tilde{y} = c$ acting as a non-compact cosmological horizon. When $b = c$, the accelerating horizon and the cosmological horizon coincide, and the above non-static region cease to exist. Finally, the region bounded by $x = -1, \tilde{y} = c$ and $\tilde{y} = -x$ is a static region from which the black hole event horizon is inaccessible. This last static region always exists.

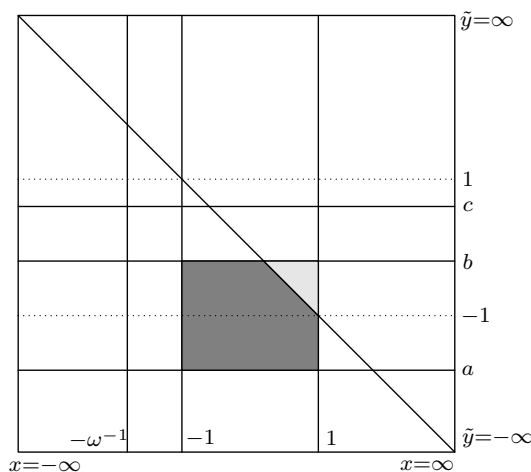


Figure 4: Static region for the case $\lambda > 0, e_2 = 0$ in the (x, \tilde{y}) subspace

At the end of this subsection, let us consider the case when $\mathcal{F}(\xi)$ has only one real root. In this case, we have $X > \frac{12(\sqrt{12\omega^2+1}+3)\omega^2+\sqrt{12\omega^2+1}-1}{54\omega^2}$, and the static region of the spacetime is bounded by the lines $x = \pm 1, \tilde{y} = a$ and $\tilde{y} = -x$, and the line $\tilde{y} = a$ still corresponds to the black hole event horizon. Diagrammatically this case corresponds to Fig.4 with the two horizontal lines $\tilde{y} = b$ and $\tilde{y} = c$ removed.

3.3 $\lambda > 0$ and $e_2 \neq 0$

Now let us consider the most general case $\lambda > 0$ with $e_2 \neq 0$. In this case, after making a coordinate reflection

$$y \rightarrow \tilde{y} = -y,$$

and repeating the process that had led to the meric form (43), we can rewrite the metric (7) as

$$ds^2 = \frac{1}{\Xi A^2(x + \tilde{y})^2} \left(\tilde{\mathcal{F}}(\tilde{y} + e_2) d\tilde{t}^2 - \frac{d\tilde{y}^2}{\tilde{\mathcal{F}}(\tilde{y} + e_2)} + \frac{dx^2}{\tilde{\mathcal{G}}(x)} + \tilde{\mathcal{G}}(x) d\tilde{\sigma}^2 \right), \quad (50)$$

where $\tilde{t} = \Xi t$, $\tilde{\sigma} = \Xi \sigma$, the constant Ξ is the same as in (42), and $\tilde{\mathcal{G}}(\xi)$, $\tilde{\mathcal{F}}(\xi)$ are still given by eqs.(44) and (45). Comparing to the case of $\lambda > 0$ with $e_2 = 0$, the only difference lies in the coordinate shifts in the metric function $\tilde{\mathcal{F}}(\tilde{y}) \rightarrow \tilde{\mathcal{F}}(\tilde{y} + e_2)$. Consequently the three roots of $\tilde{\mathcal{F}}(\tilde{y} + e_2)$ are given by

$$\tilde{y}_1 = a - e_2, \quad \tilde{y}_2 = b - e_2, \quad \tilde{y}_3 = c - e_2,$$

i.e. all three roots get shifted by the same amount $-e_2$. Since the constants a, b, c still obey the constraint (49), different amounts of shift will result in different orders of the roots $\tilde{y}_1, \tilde{y}_2, \tilde{y}_3$ when compared with the roots $x = \pm 1, -\omega^{-1}$ of $\tilde{\mathcal{G}}(x)$. Consequently, the physically interesting static region of the spacetime bounded by $x = \pm 1$ and $\tilde{y} = \tilde{y}_1, \tilde{y} = \tilde{y}_2$ and possibly the conformal infinity $\tilde{y} = -x$ will get shifted upwards or downwards as compared to the case of Fig.4. Depending on the values of e_2 and $b - a$, there are the following possibilities:

- $e_2 > 0$. Such cases are depicted in Fig.5 and the static regions are shaded in darkgray.
- $e_2 < 0$ and $b - a > 2$. Such cases are depicted in Fig.6 and the static regions are shaded in darkgray.
- $e_2 < 0$ and $b - a < 2$. Such cases are depicted in Fig.7 and the static regions are shaded in darkgray.

These figures exhaust all possible physically interesting parameter ranges of our solution when $\tilde{\mathcal{F}}(\tilde{y} + e_2)$ has three real roots. We may, of course, discuss the cases when $\tilde{\mathcal{F}}(\tilde{y} + e_2)$ has two or one real roots just like we did at the end of the last subsection. Since these cases are relatively simpler than the case with three real roots, we omit the corresponding details.

Remarks:

1. Fig.6(d) and Fig.7(d) do not contain any region shaded in darkgray, so the parameter ranges corresponding to these two figures are physically uninteresting;

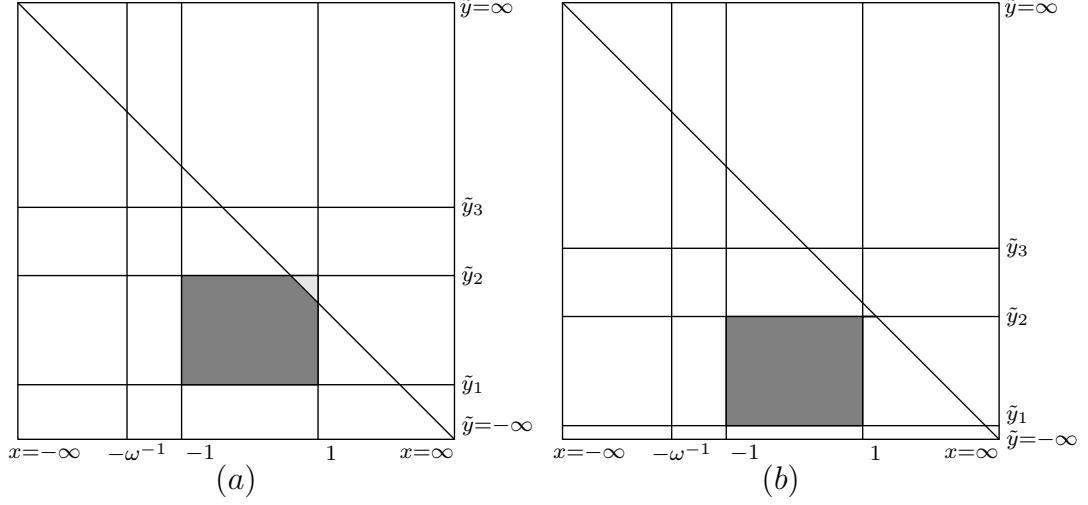


Figure 5: Static region for the case $e_2 > 0$: (a) $0 < e_2 < 1 + b$; (b) $e_2 > 1 + b$.

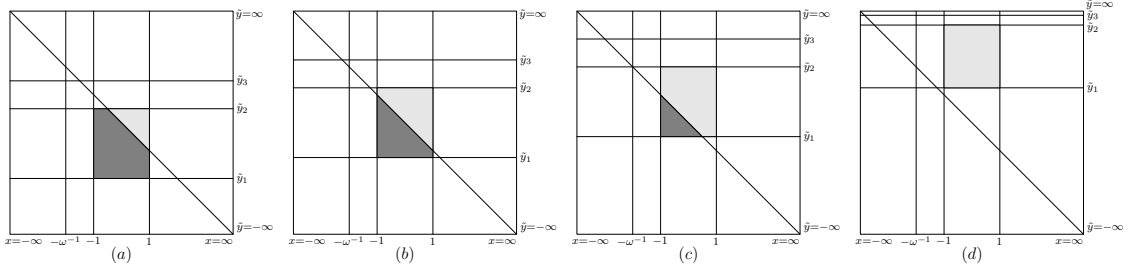


Figure 6: Static region for the case $e_2 < 0$ and $b - a > 2$: (a) $b - 1 < e_2 < 0$; (b) $a + 1 < e_2 < b - 1$; (c) $a - 1 < e_2 < a + 1$; (d) $e_2 < a - 1$.

2. In all cases in Figs.5, 6 and 7 except Fig.6(d) and Fig.7(d), the lines $\tilde{y} = \tilde{y}_1$ correspond to black hole event horizons;
3. Whenever accessible from the static region, the lines $\tilde{y} = \tilde{y}_2$ correspond to acceleration horizons and the lines $\tilde{y} = -x$ correspond to conformal infinities;
4. Some limiting cases are not depicted in Figs.5, 6 and 7. Such limiting cases occur when one or two of the corners of the rectangle bounded by $x = \pm 1$ and $\tilde{y} = \tilde{y}_1$, $\tilde{y} = \tilde{y}_2$ happen to lie on the line $\tilde{y} = -x$. In such cases, either the black hole event horizon or the acceleration horizon hit the conformal infinity at a single point;
5. In all physically interesting cases, the regions bounded by $x = \pm 1$, $\tilde{y} = \tilde{y}_1$, $\tilde{y} = -\infty$ and possibly $\tilde{y} = -x$ correspond to the black hole interior.

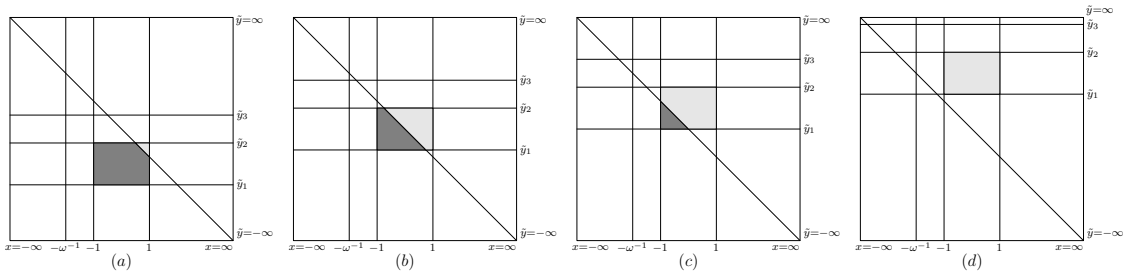


Figure 7: Static region for the case $e_2 < 0$ and $b - a < 2$: (a) $a + 1 < e_2$; (b) $b - 1 < e_2 < a + 1$; (c) $a - 1 < e_2 < b - 1$; (d) $e_2 < a - 1$.

4 Other conformal gauges

The analysis for the spacetime properties made in the last section has relied purely on the explicit form of the metric but not on the action of the CGCCS model. However, as mentioned in the introduction, an important feature of the model under study is the conformal invariance under $g_{\mu\nu} \rightarrow \Omega^2(x)g_{\mu\nu}$, $\Phi \rightarrow \Omega^{-1}(x)\Phi$, which means that if $g_{\mu\nu}$ is a solution, then $\Omega^2(x)g_{\mu\nu}$ is also a solution for any smooth function $\Omega(x)$. In this section, we would like to discuss some of the consequences or implications of the conformal invariance.

First of all, following the discussions made in the last two sections, it seems that the C-metric solution (7) with $F(y)$ and $G(x)$ given in (13), (12) does not asymptote to an (A)dS spacetime, therefore, it is not clear how to implement Maldacena's Neumann boundary condition, or whether such a boundary condition can be implemented in principle in our case. Under such circumstances, we have no other choices but considering all $\Omega(x)$ on equal footing. However, writing down the explicit form of the metric implies a concrete, fixed choice for $\Omega(x)$, i.e. we have to work in concrete conformal gauges. In fact, since the Hawking temperature of a black hole depends only on the explicit form of the metric but not on the action of the gravity model, any explicit form of the metric of a black hole spacetime implies a definite Hawking temperature and hence a prescribed energy scale, which signifies the breaking of conformal symmetry. This is the situation for all black hole solutions to conformal gravity.

Secondly, unlike the usual gauge symmetries in quantum field theories in which the gauge choice is irrelevant to the physics, different choices of conformal gauges corresponds to different physics (or physics at different scales). Another important aspect of conformal gauge choice is related to the kinematics in curved spacetime. Although the action of the model under investigation is invariant under conformal transformations, different choices of conformal gauges yield different Christoffel connections and thus different geodesics. This fact actually lies behind the reason why conformal gravity can fit the galaxy rotation curves quite good while Einstein gravity fails to do so without the introduction of dark matter [24].

Last but not the least, let us remark that unlike the situation of Einstein gravity in

which only regular conformal mappings can be applied while constructing the Carter-Penrose diagrams, in our case *any conformal factor* $\Omega^2(x)$ can be applied, even if it contains some isolated singularities, since such conformal factors do map one solution of the field equation to another². In fact, the use of singular conformal factor to map one solution of conformal gravity to another is a usual practice in the literature [25].

Among the infinite many choices of conformal gauges, we are particularly interested in two other gauge choices, which are closely related to the answer of the following two questions:

Q1. Is our solution contained in the conformal class of an Einstein manifold?

Q2. What are the major differences between all the different conformal gauges?

The answer to Q1 is simply “yes”. To see this, we would like to make a conformal transformation, bringing the original metric (7) into another conformal gauge, in which the metric becomes that of a constant curvature spacetime. Concretely, we choose the following Weyl factor $\Omega(x)$,

$$\Omega(x) = \frac{x - y}{x + y - e_2}. \quad (51)$$

Then, after performing the conformal transformation (2), the metric becomes

$$ds^2 = \frac{1}{A^2(x + y - e_2)^2} \left(-F(y)dt^2 + \frac{dy^2}{F(y)} + \frac{dx^2}{G(x)} + G(x)d\sigma^2 \right), \quad (52)$$

where $G(x)$ and $F(y)$ are still given by (12) and (13). On this occasion it is tempting to make a shift of coordinate $y \rightarrow \bar{y} = y - e_2$, after which the metric becomes

$$ds^2 = \frac{1}{A^2(x + \bar{y})^2} \left(-\bar{F}(\bar{y})dt^2 + \frac{d\bar{y}^2}{\bar{F}(\bar{y})} + \frac{dx^2}{G(x)} + G(x)d\sigma^2 \right), \quad (53)$$

where $\bar{F}(\bar{y})$ is given by

$$\bar{F}(\bar{y}) = -(1 + \bar{y})(1 - \bar{y})(1 - 2mA\bar{y}) + \frac{2e_1^2\lambda}{A^2}. \quad (54)$$

The metric (53) is precisely the AdS C-metric with the cosmological constant

$$\Lambda = -6e_1^2\lambda,$$

which appeared first in [17] and was analyzed in detail in [12, 23] in the context of standard Einstein gravity. Now we recovered the same metric in conformal gravity. The first few curvature invariants of the spacetime (54) are

$$R = -24\lambda e_1^2, \quad R_{\mu\nu}R^{\mu\nu} = 144\lambda^2 e_1^4, \quad R_{\mu\nu\rho\sigma}R^{\mu\nu\rho\sigma} = 48A^6 m^2 (x + \bar{y})^6 + 96e_1^4\lambda^2.$$

²When talking about exact solutions, one always avoids the singularities, otherwise even the Schwarzschild metric will not solve the standard Einstein equation because the metric simply loses any meaning at the singularity.

The only curvature singularity is located at $\bar{y} = \infty$. Notice that the constant e_2 disappeared completely in the metric (53). As a sharp comparison, we have seen enough on the importance of the constant e_2 while exploring the structure of the spacetime in the original gauge (7) in the last section. Notice also that after making the conformal transformation using the Weyl factor (51), the scalar field Φ in (8) becomes a constant,

$$\Phi = e_1,$$

therefore, the on-shell kinetic energy of the scalar field is zero and the on-shell scalar potential becomes an effective cosmological constant. In this case, the on-shell action of the model under investigation becomes that of the Einstein-Weyl gravity (i.e. $-R + C^2$ gravity) with a cosmological constant, which is neither that of pure Einstein gravity nor that of pure conformal gravity. Therefore, finding out that our solution to the CGCCS model lies in the conformal class of AdS C-metric is a nontrivial fact rather than just another special case that fits in Maldacena's argument for pure conformal gravity. Last but not the least, let us remark that the metric (53) looks extremely similar to the $e_2 = 0$ case of the original metric (7), however with a big difference in the position of conformal infinity. For (7), the conformal infinity lies at $y = x$, while for (53), the conformal infinity lies at $\bar{y} = -x$. So, if one intends to depict the static region of the spacetime (53), she/he would have ended in a diagram like Fig.2(a), but with the direction of the line representing conformal infinity changed from SW-NE to NW-SE.

Another conformal gauge which we would like to mention is the gauge

$$ds^2 = \frac{1}{A^2 y^2} \left(-F(y) dt^2 + \frac{dy^2}{F(y)} + \frac{dx^2}{G(x)} + G(x) d\sigma^2 \right), \quad (55)$$

which can be arrived in from (7) via the transformations

$$g_{\mu\nu} \rightarrow \frac{(x-y)^2}{y^2} g_{\mu\nu}, \quad \Phi \rightarrow \frac{y}{x-y} \Phi, \quad (56)$$

after which the scalar field takes the value

$$\Phi = \frac{e_1 y}{x + y - e_2}.$$

Notice that unlike the other two conformal gauges discussed previously, the conformal infinity in the present case appear at $y = 0$. This makes the coordinate y to be reminiscent to the famous Poincare coordinate for AdS spacetime. However, the metric (55) is not AdS, and is not even a constant curvature spacetime, as can be easily seen from the Ricci scalar

$$R = -12A^2 \left\{ mA \left[(e_2 - x)y^2 + (1 - 3e_2^2)y + 2e_2(e_2^2 - 1) \right] - e_2 y + e_2^2 - 1 \right\} - 24e_2^2 \lambda.$$

The curvature singularities appear at $|y| \rightarrow \infty$. Due to the appearance of the conformal infinity, we must take either $y \geq 0$ or $y \leq 0$ when considering the structure of the spacetime. We take the former choice $y \geq 0$.

Assuming that the ratio of parameters e_1/A is taking values in the appropriate range, we can rewrite $F(y)$ in a completely factorized form

$$F(y) = (y - a_1)(y - a_2)(\delta - 2mAy), \quad (57)$$

where a_1, a_2, δ are real numbers which are determined implicitly by the original parameters e_1, e_2, m, A . Without loss of generality, let us assume the three roots $y = a_1, a_2, a_3 \equiv \delta/(2mA)$ are ordered as

$$a_1 < a_2 < a_3.$$

Then the correct Lorentz signature of the metric requires $-1 < x < 1$ and $a_2 < y < a_3$. It can be verified using the same arguments that have led to (20) that the roots $y = a_2$ and $y = a_3$ are exactly where the proper acceleration of static observers tends to diverge. With a little bit more efforts we can identify that $y = a_3$ is the black hole event horizon and $y = a_2$ is a pure acceleration horizon, provided that these roots are accessible from the physically interesting static region of the spacetime.

Depending on the signatures of a_2 and a_3 , there are three possibilities which are depicted in Fig.8. In Fig.8(a), the physically interesting region (shaded in darkgray) is bounded by $x = \pm 1$, a black hole event horizon at $y = a_3$ and an acceleration horizon at $y = a_2$. The conformal infinity $y = 0$ lies behind the acceleration horizon and hence is out of reach from the static region. The case of Fig.8(b) is different in that the conformal infinity appears first and so the acceleration horizon is beyond reach from the static region. A possible degeneration of Fig.8(a) and Fig.8(b) occurs at $a_2 \rightarrow 0$, in which case the accelerating horizon and the conformal infinity coincide. In Fig.8(c), both $y = y_2$ and $y = y_3$ are located on the other side of the conformal infinity and therefore this case is physically uninteresting.

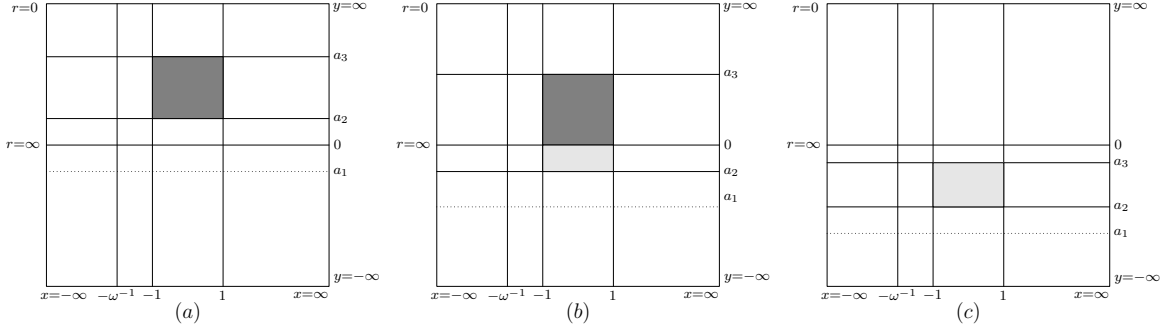


Figure 8: Static regions for the metric (55): (a) $0 < a_2 < a_3$; (b) $a_2 < 0 < a_3$; (c) $a_2 < a_3 < 0$.

If we introduce the following coordinate transformations

$$y \rightarrow \frac{1}{Ar}, \quad x \rightarrow \cos \theta, \quad t \rightarrow A\tau,$$

the metric (55) can be brought into the following form,

$$ds^2 = -\mathcal{Q}(r)d\tau^2 + \frac{dr^2}{\mathcal{Q}(r)} + \frac{r^2 d\theta^2}{\mathcal{P}(\theta)} + \mathcal{P}(\theta)r^2 \sin^2 \theta d\sigma^2, \quad (58)$$

where

$$\mathcal{Q}(r) = (1 - a_1 Ar)(1 - a_2 Ar) \left(\delta - \frac{2m}{r} \right),$$

$$\mathcal{P}(\theta) = 1 + 2mA \cos \theta.$$

In this coordinate system, the overall conformal factor in the metric completely disappeared and the metric looks like an ordinary static black hole spacetime which bears no resemblance to the C-metric. However this is only superficial. Actually, (58) still corresponds to an accelerating black hole spacetime, if the parameters are taken in the appropriate ranges. As a consequence, it can be static but not spherically symmetric unless $m = 0$.

Now reviewing the three different conformal gauges we have discussed so far, we come to the following conclusion, which is also part of the answer to Q2, i.e. the location of the conformal infinities are significantly affected by the choice of conformal gauges, and thus also the horizon structures are quite different in different conformal gauges. This is one of the major differences between different choices of conformal gauges.

5 Concluding remarks

We have thus presented an exact C-metric solution to the CGCCS model, in which the scalar field played as a nontrivial matter source. When the parameters are in the appropriate ranges, the solution may contain a black hole event horizon and an acceleration horizon and both horizons may be cut by the conformal infinity or be hidden behind the conformal infinity. The solution belongs to the class of Petrov type D spacetimes and is conformal to the standard cosmological C-metric known in vacuum Einstein gravity.

For all parameter ranges we studied in detail the physically interesting static regions as depicted in Figs.1-8 except Fig.3. However these figures do not exhaust all possible static regions. There are other static regions like the ones shaded in lightgray in the above mentioned figures in which are not of major concern in this paper. The complete understanding of the spacetime represented by our solution is still awaiting to be done, and in particular an analysis on the global structure in the new relative sense as mentioned in Sec.4 may be a good starting point. Anyway, we have seen plenty reasons to expect that the C-metric solution to the CGCCS model contain much richer physics as compared to the C-metric solution of Einstein gravity.

Acknowledgment

KM and LZ thank the anonymous referee for useful comments. This work is supported by the National Natural Science Foundation of China (NSFC) under the grant numbers 11447153 (for KM) and 11575088 (for LZ).

References

- [1] J. Maldacena, “Einstein Gravity from Conformal Gravity”, [[arXiv:1105.5632](#)].
- [2] O. Miskovic, R. Olea, “Topological regularization and self-duality in four-dimensional anti-de Sitter gravity”, *Phys. Rev. D* **79** (2009) 124020 [[arXiv:0902.2082](#)].
- [3] P. D. Mannheim and D. Kazanas, “Solutions to the Reissner-Nordström, Kerr, and Kerr-Newman problems in fourth-order conformal Weyl gravity,” *Phys. Rev. D* **44**, 417 (1991).
- [4] J. L. Said, J. Sultana, K. Z. Adami, “Charged Cylindrical Black Holes in Conformal Gravity,” *Phys. Rev. D* **86**, 104009 (2012) [[arXiv:1207.2108](#)].
- [5] Z.-Y. Fan, H. Lü, “SU(2)-Colored (A)dS Black Holes in Conformal Gravity ,” *JHEP* **1502**: 013 (2015) [[arXiv:1411.5372](#)].
- [6] T. Levi-Civita, “ ds^2 einsteiniani in campi newtoniani,” *Rend. Acc. Lincei* **27** (1918) 343.
- [7] J. Ehlers and W. Kundt, “Exact solutions of the gravitational field equations”, in *Gravitation: An Introduction to Current Research*, ed L. Witten (New York: Wiley 1962) 49-101.
- [8] H. Weyl, “Zur Gravitationstheorie”, *Ann. Phys.* **54** 117 (1917).
- [9] W. Kinnersley and M. Walker, “Uniformly Accelerating Charged Mass in General Relativity”, *Phys. Rev. D* **2** 1359-70 (1970).
- [10] W. B. Bonnor, “The sources of the vacuum C-metric”, *Gen. Rel. Grav.* **15** 535-551 (1983).
- [11] J.B. Griffiths, P. Krtous, J. Podolsky, “Interpreting the C-metric,” *Class. Quant. Grav.* **23** (2006) 6745-6766 [[arXiv:gr-qc/0609056](#)].
- [12] O. J. C. Dias, J. P. S. Lemos, “Pair of accelerated black holes in an anti-de Sitter background: the AdS C-metric,” *Phys. Rev. D* **67**, 064001 (2003) [[arXiv:hep-th/0210065](#)].
- [13] P. Krtous, “Accelerated black holes in an anti-de Sitter universe,” *Phys. Rev. D* **72**, 124019 (2005) [[arXiv:gr-qc/0510101](#)].
- [14] O. J. C. Dias, J. P. S. Lemos, “Pair of accelerated black holes in a de Sitter background: the dS C-metric,” *Phys. Rev. D* **67**, 084018 (2003) [[arXiv:hep-th/0301046](#)].
- [15] C. Charmousis, T. Kolyvaris, E. Papantonopoulos, “Charged C-metric with conformally coupled scalar field,” *Class. Quant. Grav.* **26**: 175012 (2009) [[arXiv:0906.5568](#)].
- [16] A. Anabalón, H. Maeda, “New Charged Black Holes with Conformal Scalar Hair,” *Phys. Rev. D* **81**, 041501 (2010) [[arXiv:0907.0219](#)].
- [17] J. F. Plebanski, M. Demianski, “Rotating, charged and uniformly accelerating mass in general relativity”, *Annals of Phys. (N.Y.)* 98, 98 (1976).
- [18] R. Emparan, H. S. Reall, “A rotating black ring in five dimensions,” *Phys. Rev. Lett.* **88**: 101101 (2002) [[arXiv:hep-th/0110260](#)].
- [19] R. J. Riegert, “Birkhoff theorem in conformal gravity,” *Phys. Rev. Lett.* **53**, 315 (1984).
- [20] H.-S. Liu, H. Lu, C.N. Pope, J. Vazquez-Poritz, “Not Conformally-Einstein Metrics in Conformal Gravity,” *Class. Quant. Grav.* **30**, 165015 (2013) [[arXiv:1303.5781](#)].
- [21] H. Lu, Z.-L. Wang, “Exact Green’s Function and Fermi Surfaces from Conformal Gravity,” *Phys. Lett. B* **718**, 1536-1542 (2013) [[arXiv:1210.4560](#)].
- [22] J. Li, H.-S. Liu, H. Lu, Z.-L. Wang, “Fermi Surfaces and Analytic Green’s Functions from Conformal Gravity,” *JHEP* **1302**: 109 (2013) [[arXiv:1210.5000](#)].
- [23] Y. Chen, Y.-K. Lim, E. Teo, “A new form of the C-metric with cosmological constant,” *Phys. Rev. D* **91**, 064014 (2015) [[arXiv:1501.01355](#)].

- [24] P. D. Mannheim, J. G. O'Brien, "Fitting galactic rotation curves with conformal gravity and a global quadratic potential", Phys. Rev. D.85, 124020 (2012) [[arXiv:1011.3495](#)].
- [25] H. Lu, Y. Pang, C. N. Pope and J. F. Vazquez-Poritz, "AdS and Lifshitz Black Holes in Conformal and Einstein-Weyl Gravities," Phys. Rev. D **86**, 044011 (2012) [[arXiv:1204.1062](#)].